ORFEUS II echelle spectra:
H$_2$ measurements in the Magellanic Clouds*

Ph. Richter[1,2]

[1] Sternwarte, Universität Bonn, Auf dem Hügel 71, 53121 Bonn, Germany
[2] Department of Astronomy, University of Wisconsin-Madison, Madison, WI 53706, USA

Abstract. More than 20 years after the *Copernicus* satellite, *ORFEUS* allows the investigation of molecular hydrogen (H$_2$) in the diffuse interstellar medium by way of FUV absorption spectroscopy once again. This time, targets in the Magellanic Clouds were also observed, allowing the first investigation of cold H$_2$ in a metal-poor environment outside the Milky Way disk. This paper presents new H$_2$ measurements in LMC gas along the lines of sight toward HD 269698 (Sk $-67\,166$), HD 269546 (Sk $-68\,82$) and HD 36402 (Sk $-67\,104$) and summarizes the *ORFEUS* H$_2$ measurements in the the Magellanic Clouds. For seven lines of sight we investigate correlations between $N(\mathrm{H\,I})$, $N(\mathrm{H_2})$, $E(B-V)$ and compare the results with H$_2$ observations in the Milky Way disk. We find that the abundance of H$_2$ is low in comparison to the total gas quantity and speculate that the fraction of hydrogen in molecular form is limited by the lower dust content of the Magellanic Clouds.

Key words: space vehicles – galaxies: ISM – galaxies: Magellanic Clouds – ultraviolet: ISM

1. Introduction

The molecular hydrogen (H$_2$) is by far the most abundant molecule in the interstellar medium (ISM) and thus plays a key role for our understanding of the molecular gas in the ISM of the Milky Way and other galaxies. Despite its large abundance, H$_2$ in the ISM is difficult to measure because it is not seen in radio emission, in striking contrast to the second most abundant interstellar molecule, carbon monoxide (CO). H$_2$ emission lines are seen in the near infrared (NIR), but unfortunately they are weak (quadropole transitions) and thus can not be used to study the overall interstellar abundance of H$_2$. Molecular hydrogen in the diffuse ISM can only be studied by way of absorption spectrosopy in the far ultraviolet (FUV) toward stars or other bright UV background sources. During the seventies, considerable effort was put into the investigation of H$_2$ absorption lines with the *Copernicus* satellite. Savage et al. (1977; hereafter S77) summarized *Copernicus* H$_2$ measurements of 102 lines of sight

toward nearby stars in the Milky Way. One of the most striking results was the correlation between the H$_2$ column density $N(\mathrm{H_2})$ and colour excess $E(B-V)$, representative of the dust amount along a sight line. This relation has been interpreted in terms of the self-shielding effect of H$_2$ (Federman et al. 1979). S77 showed that the transition from low to high molecular fractions in the local Galactic gas is found at total hydrogen column densities near 5.0×10^{20} cm^{-2}.

Measurements with *Copernicus*, however, were limited to the very local interstellar gas of the Milky Way. For more distant background sources, *Copernicus* was not sensitive enough. Later UV satellites, such as *IUE* and *HST*, had better sensitivity, but these instruments do not cover the wavelength range below 1150 Å where the transitions of H$_2$ are seen. The analysis of extragalactic H$_2$ gas is of great importance since the abundance of H$_2$ can be studied in environments very different from those of the Milky Way. The Magellanic Clouds, the most nearby satellite galaxies of the Milky Way, are ideal hunting grounds for extragalactic H$_2$ measurements, because they provide many bright stars suitable as UV background sources for absorption spectroscopy. Moreover, H$_2$ has been detected from warm regions in both galaxies in the near-IR emission lines (Koornneef & Israel 1985, Israel & Koornneef 1988, 1991). It has been suggested that, due to the lower metallicity and the lower dust content, the amount of H$_2$ in the diffuse interstellar medium of the Magellanic Clouds is significantly lower than in the Milky Way (Clayton et al. 1995).

The *ORFEUS* telescope, launched for its second mission in 1996, was the first instrument able to measure H$_2$ absorption lines in the LMC (de Boer et al. 1998) and SMC (Richter et al. 1998). In addition, the spectrum of LH 10:3120 was used to detemine an upper limit for the H$_2$/CO ratio in the LMC gas along this line of sight (Richter et al. 1999a). Together with the observations presented here, these *ORFEUS* spectra provide the first opportunity to investigate the relations between $N(\mathrm{H\,I})$, $N(\mathrm{H_2})$ and $E(B-V)$ in diffuse interstellar gas of the Magellanic Clouds in comparison to the Milky Way.

2. Observations

The observations have been carried out during the second mission of *ORFEUS* on the *ASTRO-SPAS* space shuttle mission

---

Table 1. Basic properties of Magellanic Cloud targets

Object Name	Other Names	Location	V [mag]	Spectral Type	$E(B-V)$ [mag]	l	b	Ref.[1]	*ORFEUS* exp. time [ksec]
LH 10:3120	...	LMC	12.80	O5.5 V	0.17	277.2	-36.1	1	6.5
HD 5980	Sk 78	SMC	11.80	OB+WN3	0.07	302.1	-44.9	2,3	6.8
HD 269698	Sk $-66\,166$	LMC	12.27	O4 If	0.09	277.8	-32.5	4,5	6.2
HD 269546	Sk $-68\,82$	LMC	11.30	B3 I+WN3	≤ 0.02	279.3	-32.8	4,6	6.4
HD 36402	Sk $-67\,104$	LMC	11.50	OB+WC5	≤ 0.02	277.8	-33.0	2,7	7.8

[1] *References:* (1) Parker et al. (1992); (2) Sembach & Savage (1992); (3) Fitzpatrick & Savage (1983); (4) Chu et al. (1994); (5) Wilcots et al. (1996); (6) Vacca & Torres-Dodgen (1990); (7) de Boer & Nash (1982) and references therein

in Nov./Dec. 1996. *ORFEUS* is equipped with two alternatively operating spectrometers, the echelle spectrometer (Krämer et al. 1990) and the Berkely spectrometer (Hurwitz & Bowyer 1996). The spectroscopic data presented here were obtained with the Heidelberg/Tübingen echelle spectrometer. This instrument has a resolution of somewhat better than $\lambda/\Delta\lambda = 10^4$ (Barnstedt et al. 1999), working in the spectral range between 912 and 1410 Å. A detailed description of the instrument is given by Barnstedt et al. (1999).

Here we study the *ORFEUS* spectra of 4 LMC stars and one SMC star. Basic information about the targets is given in Table 1. The primary data reduction was performed by the *ORFEUS* team in Tübingen (Barnstedt et al. 1999). In order to improve signal-to-noise ratios (S/N), all spectra have been filtered by a wavelet algorithm (Fligge & Solanki 1997). The resolution after filtering is $\sim 30\,\mathrm{km\,s^{-1}}$. Heliocentric velocities have been transformed for each line of sight into the LSR (Local Standard of Rest) system.

3. Data analysis

The complex line-of-sight structure in direction of the Magellanic Clouds, with contributions from local Galactic gas ($0\,\mathrm{km\,s^{-1}}$), Galactic halo gas (near $+60$ and $+120\,\mathrm{km\,s^{-1}}$ in front of the LMC) and Magellanic Cloud gas (near $+250\,\mathrm{km\,s^{-1}}$ for the LMC and $+150\,\mathrm{km\,s^{-1}}$ for the SMC; see Savage & de Boer 1979, 1981; de Boer et al. 1980; Bomans et al. 1996) makes the thorough analysis of H$_2$ absorption lines at LMC velocities and $\sim 30\,\mathrm{km\,s^{-1}}$ resolution a difficult task. The main problem is that for the vast majority of the H$_2$ transitions line blends from atomic or molecular species can not be excluded, even when many of these possible blendings are not expected. As a consequence, the number of unambigously identified H$_2$ features at high radial velocities is strongly limited to only a few wavelength regions. Typical line strengths for low H$_2$ column densities (as observed in the spectra presented in the following) have values ≤ 100 mÅ, which is (at low S/N) comparable with the strength of noise peaks. For most of these lines, only upper limits for the equivalent widths can be obtained. For diffuse H$_2$ clouds it is known that the process of UV pumping (Spitzer & Zweibel 1974) often leads to an excitation of the higher rotational states, particulary if the total H$_2$ column density is below the limit for the self-shielding effect. Thus, the rotational excitation of H$_2$ in the most diffuse medium often does *not* reflect

the actual kinetic temperature of the gas. H$_2$ line strengths in diffuse clouds for excited rotational states might be significantly higher than for the ground states (see the *Copernicus* spectrum of ζ Pup, as published by Morton & Dinerstein 1976, where the strongest H$_2$ lines occur for $J = 3$), even if the gas is cold. In the most complex case, the equivalent widths for the ground state lines are below the detection limit, while in the same spectrum, absorption from higher rotational levels is visible.

Velocity information from metal lines as well as model spectra for the excited rotational states were used to interpret the complex H$_2$ absorption pattern found in the *ORFEUS* spectra of stars in the Magellanic Clouds.

4. *ORFEUS* H$_2$ measurements

For the lines of sight toward HD 269698, HD 269546 and HD 36402 the analysis of H$_2$ line strengths is presented in the following. For 2 other lines of sight, *ORFEUS* H$_2$ measurements of Magellanic-Cloud gas have been published recently by de Boer et al. (1998; LH 10:3120) and Richter et al. (1998, 1999a; HD 5980, LH 10:3120).

Wavelengths and oscillator strengths for the H$_2$ lines have been taken from the list of Morton & Dinerstein (1976)[1]. We measured equivalent widths (W_λ) by using either trapezoidal or gaussian fits. For the error determination we used the algorithm of Jenkins et al. (1973), taking into account photon statistics and the number of pixels involved for each line. In order to estimate the uncertainty for the choice of the continuum, we fitted a maximum and a minimum continuum to the data in the vicinity of each line and derived a mean deviation. The error for W_λ given in Table 2 represents the total uncertainty calculated from all contributions discussed above. Column densities were derived by using a standard curve-of-growth technique.

4.1. HD 269698

The *ORFEUS* spectrum of HD 269698 in the Large Magellanic Cloud shows weak H$_2$ absoption at LMC velocities near $+220\,\mathrm{km\,s^{-1}}$. Six lines from the two rotational ground states ($J = 0, 1$) with high oscillator strengths are clearly seen in

---

[1] We note that the Lyman P(1), 10-0 line is located at 982.839 Å and not at 982.383 Å, as given by Morton & Dinerstein (1976). See the wavelength list of Abgrall & Roueff (1989).
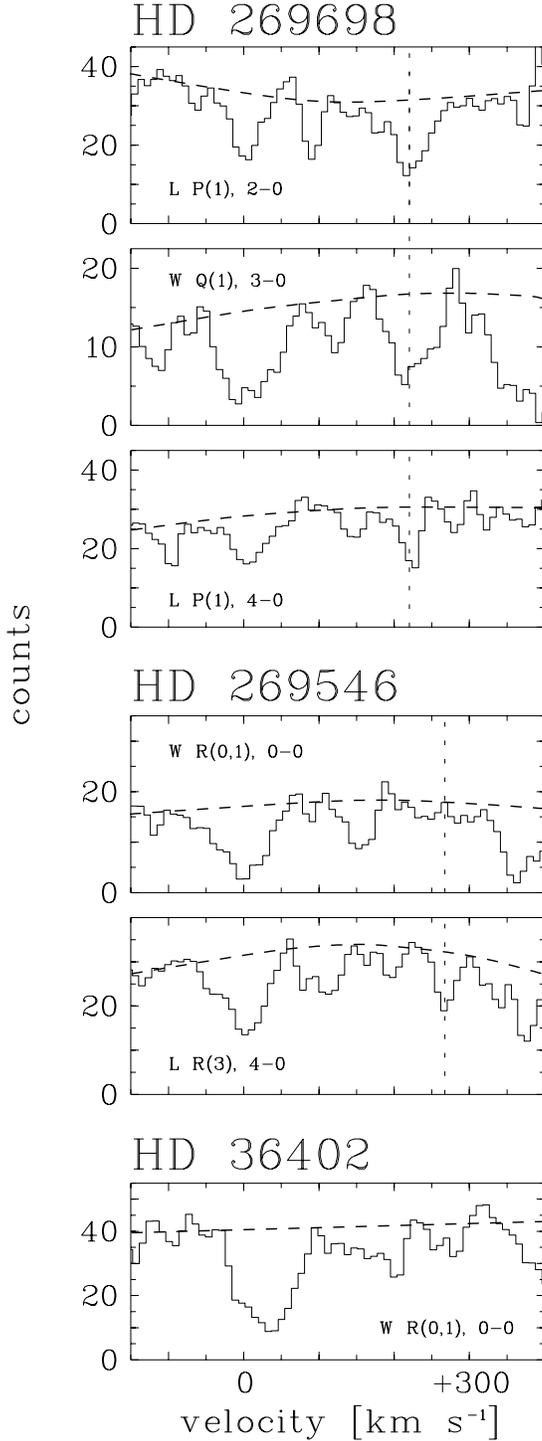
Fig. 1. Interstellar H$_2$ line profiles for HD 269698, HD 269546 and HD 36402 are shown, plotted in counts versus LSR velocity units. For HD 269698, H$_2$ absorption from LMC gas is clearly visible near $+220\,\mathrm{km\,s^{-1}}$. For HD 269546, weak H$_2$ absorption might be present near $+265\,\mathrm{km\,s^{-1}}$, but the origin of the absorption feature in the R(3), 4-0 line remains doubtful. No H$_2$ absorption at LMC velocities is seen in the *ORFEUS* spectrum of HD 36402. The LMC velocities found from the H$_2$ line centres have been marked with dashed lines. In all three spectra, H$_2$ absorption from Galactic gas is present near $0\,\mathrm{km\,s^{-1}}$. The adopted continuum is indicated for each of the profiles

Table 2. H$_2$ equivalent widths for LMC gas toward HD 269698

Line		λ [Å]	f	W [mÅ]
		$J=0, g_J=1, E_J=0\,\mathrm{eV}$		
W	R(0,1),0-0	1008.553	0.04480	present
L	R(0),2-0	1077.138	0.01190	45 ± 14
L	R(0),4-0	1049.366	0.02350	≤ 55
		$J=1, g_J=9, E_J=0.01469\,\mathrm{eV}$		
L	P(1),2-0	1078.925	0.00385	82 ± 19
L	P(1),3-0	1064.606	0.00584	≤ 82
L	R(1),4-0	1049.958	0.01600	88 ± 25
L	P(1),4-0	1051.031	0.00749	77 ± 25
W	Q(1),3-0	947.425	0.02730	111 ± 26
		$J=2, g_J=5, E_J=0.04394\,\mathrm{eV}$		
L	R(2),4-0	1051.497	0.01470	≤ 34
W	Q(2),0-0	1010.941	0.02380	≤ 59
		$J=3, g_J=21, E_J=0.08747\,\mathrm{eV}$		
L	R(3),4-0	1053.976	0.01420	≤ 47

the spectrum and are not blended by other transitions. For additional five lines from higher rotational states we find upper limits for the equivalent widths of $W_\lambda \leq 82\,\mathrm{mÅ}$ (Table 2). Fig. 1 shows three of the detected H$_2$ absorption lines plotted on a velocity scale. The lack of absorption in higher rotational states indicates that the H$_2$ gas is not strongly excited. Constructing curves of growth for each rotational state we obtain column densities of $4.0^{+4.0}_{-2.0} \times 10^{14}\,\mathrm{cm^{-2}}$ for $J=0$ and $5.0^{+6.0}_{-3.0} \times 10^{15}\,\mathrm{cm^{-2}}$ for the $J=1$ state, using a b value of $8\,\mathrm{km\,s^{-1}}$ (best fit). The total H$_2$ column density in the LMC gas toward HD 269698, derived by summing over $N(0)$ and $N(1)$, is $N(\mathrm{H_2})_{\mathrm{total}} = 5.4^{+7.3}_{-3.1} \times 10^{15}\,\mathrm{cm^{-2}}$. The error is derived from the uncertainty for the fit to the curve of growth and includes the error for the individual equivalent widths and the uncertainty for the b value. From the detection limits for the lines from $J \geq 2$ we can exclude the possibilty that the higher rotational states will significantly contribute to the total H$_2$ column density.

HD 269698 is located in the OB association N 57 at the rim of the supergiant shell LMC 4 where the H I emission (Rohlfs et al. 1984) has a minimum. The *IUE* spectrum of HD 269698 (Domgörgen et al. 1994) reveals three S II components at LMC velocities in front of the star: near $+220\,\mathrm{km\,s^{-1}}$, near $+245\,\mathrm{km\,s^{-1}}$ and near $+290\,\mathrm{km\,s^{-1}}$. The detected H$_2$ lines obviously belong to the first component.

4.2. HD 269546

In the *ORFEUS* spectrum of the LMC star HD 269546, no clear H$_2$ absorption is visible at LMC velocities. The presence of H$_2$ at LMC velocities (near $+200\,\mathrm{km\,s^{-1}}$) in *ORFEUS* data was indicated by Widmann et al. (1998), using a coaddition of 25 Lyman- and Werner lines. However, the Werner R(0), R(1) line-

Table 3. LMC gas properties along seven lines of sight

Object	Location	$E(B-V)_{\rm LMC}$ [mag]	$\log N({\rm H_2})$	$\log N({\rm H\,I})$	$N({\rm H\,I}+{\rm H_2})/E(B-V)$ [cm^{-2}]	$\log f$	Ref.[2]
LH 10:3120	LMC	0.12 ± 0.03	18.8 ± 0.3[1]	$21.3^{+0.2}_{-0.4}$	1.7×10^{22}	-2.18	1,2
HD 5980	SMC	0.05 ± 0.02	16.7 ± 0.4[1]	21.0 ± 0.2	2.0×10^{22}	-4.00	3,4
HD 269698	LMC	$0.02^{+0.03}_{-0.02}$	15.7 ± 0.4[1]	20.3 ± 0.1	1.0×10^{22}	-4.27	5
HD 269546	LMC	≤ 0.03	≤ 15.4	20.3 ± 0.1	$\geq 6.7 \times 10^{21}$	≤ -4.64	5
HD 36402	LMC	≤ 0.03	≤ 15.0	$20.2^{+0.1}_{-0.2}$	$\geq 5.3 \times 10^{21}$	≤ -4.89	5,6
Sk $-66\,19$	LMC	0.25 ± 0.03	20.2 ± 0.1[3]	$21.9^{+0.2}_{-0.3}$	3.0×10^{22}	-1.37	7,8
Sk $-69\,270$	LMC	0.19 ± 0.03	19.9 ± 0.2[3]	$21.5^{+0.2}_{-0.3}$	1.9×10^{22}	-1.41	7,8

[1] Errors include uncertainty for the choice of the doppler parameter b

[2] References: (1) de Boer et al. (1998); (2) Richter et al. (1999a); (3) Richter et al. (1998); (4) Fitzpatrick & Savage (1983); (5) this paper; (6) de Boer & Nash (1982); (7) Gunderson et al. (1998); (8) Fitzpatrick (1985)

[3] From intermediate resolution spectra with *HUT*

pair near 1009 Å (in Fig. 1 plotted on a velocity scale) gives no hint for the presence of H$_2$ absorption at LMC velocities. Marginal H$_2$ absorption might be present in the Lyman P(1), 2-0 line ($\lambda = 1078.925$ Å) and in the Lyman R(3), 4-0 line ($\lambda = 1053.976$ Å) near $+265$ km s^{-1} (Fig. 1), but these absorption features are not clearly distinguishable from noise peaks and no other H$_2$ profiles from $J = 1, 3$ show similar features at $+265$ km s^{-1}. Metal lines in the LMC gas near $+250$ km s^{-1} have been found in the *IUE* spectrum of HD 269546 (Grewing & Schulz-Luepertz 1980). Moreover, the *IUE* data reveal absorption over the whole velocity range between 0 and $+290$ km s^{-1}, most likely related to Galactic halo gas and weaker LMC components. H$_2$ absorption at $+120$ km s^{-1} is seen in some of the stronger lines, indicating that the Galactic high-velocity gas in front of HD 269546 contains molecular gas and dust (Richter et al. 1999b). The H I emission line data from Rohlfs et al. (1984) show the LMC gas at $+250$ km s^{-1}. HD 269546 is member of the OB association LH 58 in the N 144 superbubble complex northwest of 30 Doradus. The H I gas seen in 21 cm emission at $+250$ km s^{-1} is most likely in front of N 144.

Detection limits for eight H$_2$ absorption lines at LMC velocities near $+265$ km s^{-1} are used to obtain upper limits for the column densities of $N(J)$ for $J \leq 4$ by fitting the values of $\log (W_\lambda/\lambda)$ to the linear part of the curve of growth. We calculate an upper limit for the total H$_2$ column density by modeling the population of the rotational states for $T_{\rm ex} \leq 300$ K. From that we derive $N({\rm H_2})_{\rm total} \leq 2.3 \times 10^{15}$ cm^{-2} for the LMC gas toward HD 269546.

4.3. HD 36402

No H$_2$ absorption is seen in the spectrum of HD 36402 at LMC velocities in the range $+220$ to $+320$ km s^{-1}. In this velocity range, atomic absorption has been found by de Boer & Nash (1982). We place an upper limit on the H$_2$ column density in the LMC gas after inspecting some of the strongest of the H$_2$ transitions in the rotational states $J = 0$ to $J = 4$. HD 36402 is located in the superbubble N 51D and shows hydrogen emission and metal absorption from LMC foreground gas near $+300$ km s^{-1} (de Boer & Nash 1982). Therefore we

expect H$_2$ absorption from LMC gas roughly at the same velocity. Inspecting the R(0), R(1) line-pair near 1009 Å plotted on the velocity scale (Fig. 1, lowest panel), we find weak absorption near $+290$ km s^{-1}, but this feature has no significance with respect to the noise.

In the same way as for HD 269546, we determine upper limits for the individual column densities $N(J)$ for $J \leq 4$ from the detection limits for some of the stronger H$_2$ transitions near $+300$ km s^{-1}. We find an upper limit for the total H$_2$ column density in the LMC gas toward HD 36402 of $N({\rm H_2})_{\rm total} \leq 1.0 \times 10^{15}$ cm^{-2}. Again, this upper limit is calculated under the assumption that the excitation temperature of possibly existing H$_2$ gas in the LMC would not exceed a value of 300 K.

5. H I measurements

For two of our sight lines (HD 269698 and HD 269546) we present the determination of H I column densities from the analysis of the Ly α absorption near 1215 Å. The values for the H I column densities along the other three lines of sight have been adopted from the literature. All H I column densities are summarized in Table 3. For HD 5980 and HD 36402, the column density of H I has been determined by Fitzpatrick & Savage (1983) and de Boer & Nash (1982), respectively, using H I emission line data in combination with the Ly α absorption near 1215 Å. They derive H I column densities of $N({\rm H\,I}) = 1.0 \times 10^{21}$ cm^{-2} for the SMC gas toward HD 5980 and 1.6×10^{20} cm^{-2} for the LMC gas toward HD 36402. For LH 10:3120, the LMC H I column density is 2.0×10^{21} cm^{-2}, obtained by a multi-component fit of the Ly α profile (Richter et al. 1999a).

We use a similar technique for the determination of H I column densities in the LMC gas toward HD 269698 and HD 269546. For HD 269546, we fix the LMC component at a velocity of $+265$ km s^{-1}, similar to the velocity for which we had determined the upper limit for the H$_2$ column density in Sect. 4.2. The velocity structure seen in metal lines (Grewing & Schulz-Luepertz 1980), however, indicates that there are definitely additional (weaker) absorption components in front of HD 269546. We thus might slightly overestimate the H I column density in the LMC gas at $+265$ km s^{-1} by fitting one
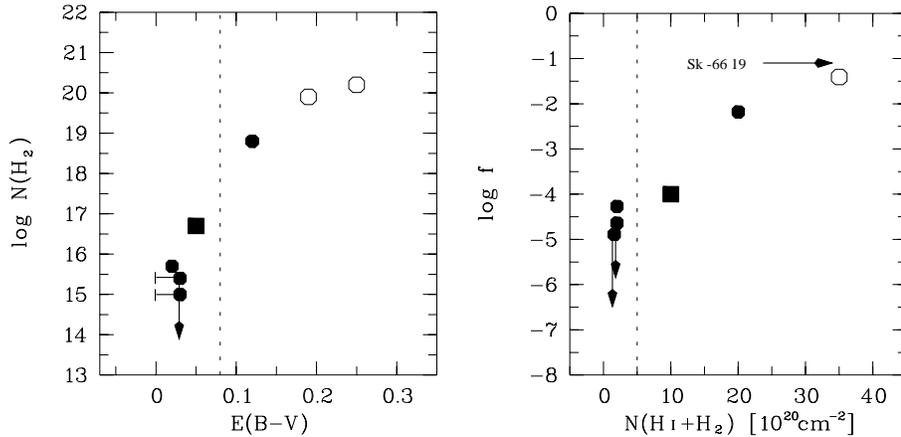
Fig. 2. Correlations between atomic hydrogen, molecular hydrogen and colour excess for Magellanic Cloud gas along seven lines of sight. LMC stars measured with *ORFEUS* are labeled by filled dots, the one SMC target is given by a filled square. Data from Gunderson et al. (1998) for two additional lines of sight to the LMC have been included, here given as open circles. The plots are discussed in Sect. 7

single LMC component to the Ly α absorption structure. The situation is even more difficult for the Ly α profile in the spectrum of HD 269698. *IUE* data of HD 269698 show the presence of three velocity components in this sight line (Domgörgen et al. 1994), near $+220$, $+245$ and $+290 \, \text{km s}^{-1}$. The H I emission (Rohlfs et al. 1984) shows a weak component near $+256 \, \text{km s}^{-1}$ which could be associated with the absorption component near $+245 \, \text{km s}^{-1}$ (see Domgörgen et al. 1994). The S II abundances found by Domgörgen et al. indicate similar total gas quantities for the two main components at $+245 \, \text{km s}^{-1}$ and $+220 \, \text{km s}^{-1}$. The H₂ absorption was found in the latter component (see Sect. 4.1). For the Ly α fit, we fix the two LMC components at $+220$ (cloud I) and $+245$ (cloud II) km s^{-1}, assuming equal H I column densities. For the fitting procedure we use a multi-component Voigt profile. Galactic foreground absorption by H I is taken into account by a fit component at $0 \, \text{km s}^{-1}$. The multiple velocity components are not resolved in the Ly α profile and we do not take into account additional absorption from Galactic intermediate and high-velocity gas. Thus, it is clear that our results derived by this method represent only rough estimates for the distribution of the H I gas in front of the stars. However, for the comparison between $N(\text{H I})$, $N(\text{H}_2)$ and $E(B-V)$, as presented in Sect. 7, the determined H I column densities are sufficiently accurate.

The Ly α fit for HD 269546 provides the best agreement with the data with a Galactic foreground absorption of $N(\text{H I})_{\text{MW}} = 3.5 \pm 0.6 \times 10^{20} \, \text{cm}^{-2}$ and an additional LMC component at $+265 \, \text{km s}^{-1}$ of $N(\text{H I})_{\text{LMC}} = 2.0 \pm 0.5 \times 10^{20} \, \text{cm}^{-2}$. For HD 269698, the best fit is found for $N(\text{H I})_{\text{MW}} = 3.5 \pm 0.7 \times 10^{20} \, \text{cm}^{-2}$ and $N(\text{H I})_{\text{LMC,comp. I}} \equiv N(\text{H I})_{\text{LMC,comp. II}} = 1.0 \pm 0.4 \times 10^{20} \, \text{cm}^{-2}$ for the two LMC clouds at $+220$ and $+245 \, \text{km s}^{-1}$. The H I column densities in the LMC gas in these two lines of sight are significantly lower than found for HD 5980 and LH 10:3120, but comparable with the H I column density found in the LMC gas toward HD 36402.

6. Colour excess $E(B-V)$

The colour excess $E(B-V)$ for each line of sight, adopted from different publications, is given in Table 1. All lines of sight show total values of $E(B-V)$ lower than 0.20 mag. The main

problem is to separate the contributions of the Galactic foreground from the colour excess within the Magellanic Clouds. For LH 10:3120 (LMC) and HD 5980 (SMC), we adopt values for $E(B-V)_{\text{LMC}}$ from previous publications (de Boer et al. 1998; Richter et al. 1998). For HD 269698 and HD 269546, we have calculated the foreground extinction from the H I column densities of the Galactic foreground gas by using the mean gas-to-colour excess relation, as given by Bohlin et al. (1978). The values for $E(B-V)_{\text{LMC}}$ are presented in Table 3. Their errors are based on the uncertainty for $E(B-V)_{\text{total}}$ (as cited in the literature; see Table 1) in addition to the uncertainty for the Galactic foreground reddening, which shows variations in the range of 0.05 mag in direction of the LMC and 0.02 mag toward the SMC (Bessel 1991).

7. Discussion

Values of $N(\text{H I})$, $N(\text{H}_2)$ and $E(B-V)$ for all five lines of sight measured with *ORFEUS* (summarized in Table 3) are used to investigate the diffuse molecular ISM of the Magellanic Clouds. In order to extend our data, we include recent results from Gunderson et al. (1998) for two lines of sight toward Sk $-66\,19$ and Sk $-69\,270$ in the LMC. They estimate, on the basis of low dispersion spectra with the Hopkins Ultraviolet Telescope (*HUT*), column densities of molecular hydrogen in the LMC gas by fitting H₂ line profiles (see Table 3).

Fig. 2 presents correlations between $N(\text{H}_2)$, $E(B-V)$, $f = 2N(\text{H}_2)/[N(\text{H I})+2N(\text{H}_2)]$, and $N(\text{H I}+\text{H}_2) = N(\text{H I}) + 2N(\text{H}_2)$. The left panel shows log $N(\text{H}_2)$ plotted versus $E(B-V)$. In principle, we find the typical relation known from the *Copernicus* H₂ survey from S77 for Galactic gas. In both Milky Way and the Magellanic Clouds the logarithmic H₂ column density (log $N(\text{H}_2)$) undergoes a transition from low to high values at $E(B-V) \approx 0.08$ (dashed line) due to the self-shielding effect of H₂ (Federman et al. 1979).

It is known that the Magellanic Clouds have a significantly lower dust content than the Milky Way. Typical gas-to-dust ratios $N(\text{H I}+\text{H}_2)/E(B-V)$ in the Magellanic Clouds are 4 times (LMC) and 8 times (SMC) higher than in Milky Way gas (Koornneef 1982; Bouchet et al. 1985, respectively). In our sample, we find gas-to-dust ratios as high as $3.0 \times 10^{22} \, \text{cm}^{-2}$

for the gas in the LMC and SMC (see Table 3), consistent with these results. For HD 36402, HD 269698 and HD 269546, the ratios are significantly lower, but note that these values most likely represent lower limits due to the large uncertainty for the gas-to-dust ratio near the zero point of the $E(B-V)$ scale. With respect to the generally lower dust content and the relation between H$_2$ column density and $E(B-V)$ (Fig. 2, left panel) one should expect that the fraction of gas in molecular form is significantly lower in the Magellanic Cloud than in the Milky Way. From more theoretical considerations, Elmegreen (1989) concluded that interstellar clouds in Magellanic type irregular galaxies should be mostly atomic, since their lower metallicity directly influences the shielding function S for the cloud layers. This author also showed that the H to H$_2$ conversion also depends sensitively on the pressure and radiation field in the ISM (Elmegreen 1993). Accordingly, typical sight lines through the Magellanic Clouds might not contain any measureable column density of H$_2$, except for those, whose column density in H I is high enough to allow a significant fraction of the hydrogen to convert into molecular form. As the right panel of Fig. 2 shows, the discussed effects are slightly visible in the FUV absorption line data. The figure shows the molecular fraction f plotted against the total hydrogen column density N(H I+H$_2$). The *Copernicus* sample (S77) shows that the transition from low ($f \leq 10^{-2}$) to high ($f > 10^{-2}$) molecular fractions in the local Galactic gas is found at a total hydrogen column density ('transition column density' N_T(H I)) near 5.0×10^{20} cm^{-2} (right panel, dashed line). We find high total hydrogen column densities ($\geq 10^{21}$ cm^{-2}) but low molecular hydrogen fractions ($f \leq 10^{-2}$) for the Magellanic Clouds gas along two of seven lines of sight. The data points of these two lines of sight toward LH 10:3120 and HD 5980 indicate that the transition column density N_T from low to high molecular fractions could be indeed higher in the Magellanic Clouds than in the Milky Way. Only for sight lines with a very high total hydrogen column density (Sk $-66\,19$ and Sk $-69\,270$), the molecular fractions exceeds values above 1 percent. For sight lines with N(H$_{total}$) $\leq 10^{21}$ cm^{-2} the molecular fractions in the Magellanic Cloud gas seem to be negligible.

Additional sight line measurements toward the Magellanic Clouds, however, are required to investigate these relations on a statistically more significant level. With a larger data set it might be possible to determine the transition column density from low to high molecular fractions as a function of the overall metallicity. Since it is known that the SMC is even more metal-poor than the LMC, it is of special interest to also investigate differences in the molecular gas fractions between LMC and SMC. For that, the *FUSE* satellite, launched in June 1999, holds the prospect for fresh H$_2$ absorption line data in the near future.

References

Abgrall H., Roueff E., 1989, A&AS 79, 313
Barnstedt J., Kappelmann N., Appenzeller I., et al., 1999, A&AS 134, 561
Bessel M.S., 1991, A&A 242, L17
Bohlin R.C., Savage B.D., Drake J.F., 1978, ApJ 224, 132
Bomans D.J., de Boer K.S., Koornneef J., Grebel E.K., 1996, A&A 313, 101
Bouchet P., Lequeux J., Maurice E., Prevot L., Prévot-Burnichon M.L., 1985, A&A 149, 330
Chu Y., Wakker B., Mac Low M., et al., 1994, AJ 108, 169
Clayton G.C., Green J., Wolff M.J., et al., 1995, ApJ 460, 313
de Boer K.S., Koornneef J., Savage B.D., 1980, ApJ 236, 769
de Boer K.S., Nash A.G., 1982, ApJ 255, 447
de Boer K.S., Richter P., Bomans D.J., Heithausen A., Koornneef J., 1998, A&A 338, L5
Domgörgen H., Bomans D.J., de Boer K.S., 1994, A&A 296, 523
Elmegreen B.G., 1989, ApJ 338, 178
Elmegreen B.G., 1993, ApJ 411, 170
Federman S.R., Glassgold A.E., Kwan J., 1979, ApJ 227, 466
Fitzpatrick E.L., 1985, ApJ 299, 219
Fitzpatrick E.L., Savage B.D., 1983, ApJ 267, 93
Fligge M., Solanki S.K., 1997, A&AS 124, 579
Grewing M., Schulz-Luepertz E., 1980, in: 'Proc. of the second *IUE* conference', ESA SP-157, 357
Gunderson K.S., Clayton G.C., Green J.C., 1998, PASP 110, 60
Hurwitz M., Bowyer S., 1996, in: Bowyer S., Malina R.F. (eds.), Astrophysics in the extreme ultraviolet. Kluwer. p. 601
Israel F.P., Koornneef J., 1988, A&A 190, 21
Israel F.P., Koornneef J., 1991, A&A 248, 404
Jenkins E.B., Drake J.F., Morton D.C., et al., 1973, ApJ 181, L122
Koornneef J., 1982, A&A 107, 247
Koornneef J., Israel F.P., 1985, ApJ 291, 156
Krämer G., Barnstedt J., Eberhard N., et al., 1990, in: Kondo Y. (ed.), Observatories in Earth Orbit and Beyond, Ap. Sp. Sci. Lib., Vol. 166. Kluwer, p. 177
Morton D.C., Dinerstein H.L., 1976, ApJ 204, 1
Parker J.W., Garmany C.D., Massey P., Walborn N.R., 1992, AJ 103, 1205
Richter P., Widmann H., de Boer K.S., et al., 1998, A&A 338, L9
Richter P., de Boer K.S., Bomans D.J., et al. 1999a, A&A 351, 323
Richter P., de Boer K.S., Widmann H., et al., 1999b, Nat 402, 386
Rohlfs K., Kreitschmann J., Siegman B.C., Feitzinger J.V., 1984, A&A 137, 343
Savage B.D., de Boer K.S., 1979, ApJ 230, L77
Savage B.D., de Boer K.S., 1981, ApJ 243, 460
Savage B.D., Bohlin R.C., Drake J.F., Budich W., 1977, ApJ 216, 291 (S77)
Sembach K.R., Savage B.D., 1992, ApJS 83, 147
Spitzer L., Zweibel E.G., 1974, ApJ 191, L127
Vacca W.D., Torres-Dodgen A.V., 1990, ApJS 1990, 658
Widmann H., Krämer G., Appenzeller I., et al., 1998, in: Breitschwerdt D., Freyberg M.J., Truemper J. (eds.), IAU Coll. 166, The local bubble and beyond, Springer, p. 517
Wilcots E.M., Hodge P.W., King N., 1996, ApJ 458, 580